*J. Fluid Mech.* (1984), *vol.* 145, *pp.* 201–221
*Printed in Great Britain*



# The motion of a small sphere in fluid near a circular hole in a plane wall

By TAKESHI MIYAZAKI
Division of Atmospheric Environment, The National Institute for Environmental Studies, Tsukuba, Ibaraki, Japan

AND HIDENORI HASIMOTO
Department of Physics, University of Tokyo, Japan

(Received 12 July 1983 and in revised form 14 March 1984)

The Stokes flow due to the motion of a small particle in arbitrary directions is investigated in the presence of a circular hole in an infinite thin plane wall separating a quiescent viscous fluid.

The solutions of the boundary-value problem are obtained in closed forms to the point-force approximation in toroidal coordinates, by the use of the Green and Neumann functions supplemented by the edge function to remove the singularity at the rim of the hole. The volume flux through the hole and the force and torque experienced by the small spherical particle are determined on the basis of this solution. The case of linear motion parallel to the plane of the wall is discussed in detail.

## 1. Introduction

The motion of a small particle near an orifice is an interesting problem with various biological and engineering applications. Recently, the axisymmetric motion near a circular hole in a thin plane wall has been studied on the basis of the point force (Stokeslet) approximation (Hasimoto 1979, 1981; Davis, O'Neill & Brenner 1981). Dagan, Weinbaum & Pfeffer (1982) presented the general theory for the motion of a sphere of arbitrary size by the use of two series solutions in two semi-infinite domains and the collocation technique.

The non-axisymmetric solution for the Stokeslet perpendicular to the plane wall has been presented by Miyazaki & Hasimoto (1982) in terms of the Green function, yielding a singularity on the rim of the hole, which can be removed by the complementary infinite-series solution.

Recently, a closed-form solution for arbitrary direction of the Stokeslet has been given by Hasimoto, Kim & Miyazaki (1983) in the case of a semi-infinite plate, yielding the approximation for the Stokeslet in the vicinity of a circular hole, where the convergence of the infinite series is slow.

In this paper the solution for the circular hole will be given in closed form for a Stokeslet of arbitrary position and direction.

Fundamental equations and the outline of the method of solution will be presented in §§2 and 3. The solution is given in terms of the Green and Neumann functions supplemented by the edge function to remove the singularity on the rim of the hole. Toroidal coordinates are adopted.

In §4 these solutions are applied to the case of a small sphere translating in a quiescent fluid. In §4.1 the volume flux through the hole is given by contours referred

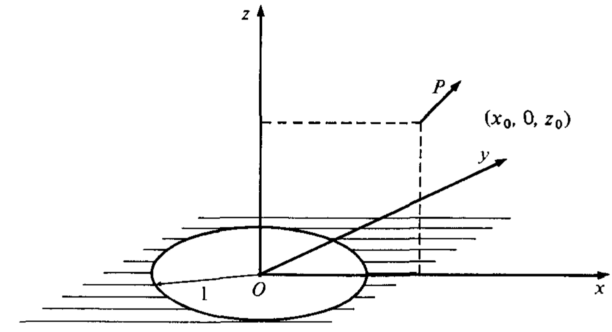


FIGURE 1. Geometry of the problem.

to the position of the sphere. In §4.2 the drag, sideforce and torque on the particle are given to first order in the wall effect. They are given in terms of tensor coefficients, whose values are presented as contours referring to the position of the particle. As an example, the case of the translation along a line parallel to the wall is studied in detail.

## 2. Fundamental equations

Let us consider a viscous fluid separated by the plane $z = 0$ with a circular hole of radius unity, whose centre is at the origin of the cylindrical coordinate system $(\rho, \theta, z)$. Figure 1 shows the geometry of the problem. We also make use of the Cartesian coordinates $(x, y, z)$ with unit vectors $\hat{\boldsymbol{x}}$, $\hat{\boldsymbol{y}}$ and $\hat{\boldsymbol{z}}$ parallel to each axis, and with

$$x = \rho\cos\theta, \qquad y = \rho\sin\theta. \tag{2.1),(2.2}$$

A small particle at $x_0 = (x_0, 0, z_0)$ translating in an arbitrary direction induces a flow in the fluid, which is at rest at infinity.

On the assumption that the particle is small and that its motion is slow, we have the following equations of motion (2.3) and of continuity (2.4), i.e. we adopt the Stokes equation of motion:

$$\operatorname{grad} p = \mu\nabla^2 \boldsymbol{v}, \qquad \operatorname{div} \boldsymbol{v} = 0, \tag{2.3), (2.4}$$

where $p$ is the pressure, $\boldsymbol{v} = (u, v, w)$ the velocity, $\mu$ the viscosity coefficient and $\nabla^2 = \partial^2/\partial x^2 + \partial^2/\partial y^2 + \partial^2/\partial z^2$ denotes the Laplacian operator.

The boundary conditions on the rigid wall are given by

$$\boldsymbol{v} = 0 \quad \text{on} \quad z = 0,\ \rho > 1 \quad \text{and} \quad \boldsymbol{v} \to 0 \quad \text{as} \quad |x| \to \infty. \tag{2.5), (2.6}$$

Assuming that the particle size is far smaller than the distance from the wall, we place at the particle position Stokeslet singularities, which play the role of driving forces with a unit strength.

Owing to the linearity of the problem we have only to study the three cases where the direction of the Stokeslet is parallel to each coordinate axis (denoted by $x_j$ ($j = 1, 2, 3$) for $x$, $y$, $z$ respectively):

$$8\pi\mu \boldsymbol{v}^{(j)} = \boldsymbol{q}_{\mathrm{S}}^{(j)} = \mathbf{O}_j\left[\frac{1}{R}\right] - x_{j0}\operatorname{grad}\left(\frac{1}{R}\right), \tag{2.7}$$

$$4\pi p = p_{\mathrm{S}}^{(j)} = \frac{\partial(1/R)}{\partial x_j}, \tag{2.8}$$

where

$$R = |x - x_0|, \tag{2.9}$$

is the distance from $\boldsymbol{x}_0$ and $\mathbf{O}_j$ denotes the operator

$$\mathbf{O}_j[\phi] = x_j \operatorname{grad} \phi - \phi \hat{\boldsymbol{x}}_j, \tag{2.10}$$

yielding the Stokes velocity from the harmonic function satisfying

$$\nabla^2 \phi = 0. \tag{2.11}$$

The outline of the method of solution and the exact solution for each case by this method will be presented in the following sections.

## 3. Outline of the method of solution

The general solution of the Stokes equation is given by four harmonic functions $\phi_i$ $(i = 1, 2, 3, 4)$ as follows (see e.g. Hasimoto & Sano 1980):

$$8\pi\mu \boldsymbol{v} = \sum_{i=1}^{3} \mathbf{O}_i[\phi_i] + \operatorname{grad} \phi_4 \quad \text{and} \quad 4\pi p = \sum_{i=1}^{3} \frac{\partial \phi_i}{\partial x_i}. \tag{3.1), (3.2}$$

These functions should be determined from the boundary conditions (2.5)–(2.8).

In our problem it is rather convenient and simple to introduce the Green and the Neumann functions $G$ and $H$ to satisfy the boundary conditions, and to remove the edge singularity at the rim of the hole $\rho = 1, z = 0$ by introducing the complementary singular solutions later on.

Let us introduce the toroidal coordinates $(\xi, \theta, \eta)$ related to $(\rho, \theta, z)$ by

$$\rho = \frac{\operatorname{sh} \xi}{\operatorname{ch} \xi - \cos \eta} \tag{3.3}$$

and

$$z = \frac{\sin \eta}{\operatorname{ch} \xi - \cos \eta} \quad (0 < \xi < \infty,\ 0 \leqslant \eta \leqslant 2\pi), \tag{3.4}$$

where the wall is given by $\eta = 0$ and $2\pi$, and $\xi = \infty$ corresponds to the rim of the hole. Then $G$ and $H$ are given by (Wendt 1958),

$$G = \tfrac{1}{2}(W - W^*) \quad \text{and} \quad H = \tfrac{1}{2}(W + W^*), \tag{3.5), (3.6}$$

where

$$W = \frac{1}{R}\left[1 + \frac{2}{\pi} \sin^{-1} \frac{\cos \frac{1}{2}(\eta - \eta_0)}{\operatorname{ch} \frac{1}{2} w}\right], \tag{3.7}$$

$$R = \frac{[2 \operatorname{ch} w - 2 \cos(\eta - \eta_0)]^{\frac{1}{2}}}{M_0 M}, \tag{3.8}$$

$$M = M(\xi, \eta) = (\operatorname{ch} \xi - \cos \eta)^{\frac{1}{2}}, \quad M_0 = M(\xi_0, \eta_0), \tag{3.9}$$

$$\operatorname{ch} w = \operatorname{ch} \xi \operatorname{ch} \xi_0 - \operatorname{sh} \xi \operatorname{sh} \xi_0 \cos \theta, \tag{3.10}$$

and the quantities with the asterisk $*$ are obtained by replacing $\eta_0$ by $-\eta_0$ in corresponding quantities. According to the definitions of $G$ and $H$,

$$\tilde{G} = G - \frac{1}{R} \quad \text{and} \quad \tilde{H} = H - \frac{1}{R} \tag{3.11}$$

are regular harmonic functions in the flow field,

$$\nabla^2\tilde{G} = 0, \quad \nabla^2\tilde{H} = 0, \tag{3.12}$$

and satisfy the boundary conditions

$$\tilde{G} = -\frac{1}{R}, \quad \frac{\partial\tilde{H}}{\partial z} = -\frac{\partial}{\partial z}\left(\frac{1}{R}\right),$$

i.e.

$$G = 0, \quad \frac{\partial H}{\partial z} = 0 \quad \text{at } z = 0, \quad \rho > 1 \quad (\text{i.e. } \eta = 0, 2\pi). \tag{3.13}$$

Letting $\xi \to \infty$ in (3.5)–(3.10), the behaviour of $G$ and $\tilde{H}$ at the edge of the hole is found to be

$$\frac{G}{\sin\frac{1}{2}\eta_0 \sin\frac{1}{2}\eta} = \frac{\tilde{H}}{\cos\frac{1}{2}\eta_0\cos\frac{1}{2}\eta} = \frac{2^{\frac{3}{2}}}{\pi} M_0\,\psi(\theta)\,\mathrm{e}^{-\frac{1}{2}\xi}\left(1+O(\mathrm{e}^{-\xi})\right)$$

$$= \frac{2}{\pi}\frac{M_0}{M}\psi(\theta)\left(1+O(\mathrm{e}^{-\xi})\right), \tag{3.14}$$

where

$$\psi(\theta) = (\operatorname{ch}\xi_0 - \operatorname{sh}\xi_0\cos\theta)^{-1}. \tag{3.15}$$

If we replace $1/R$ by $G$ in (2.7) and (2.8) and add a particular solution $\mathbf{O}_3[\phi_j]$ in terms of a harmonic function $\phi_j$, we have

$$8\pi\mu\mathbf{v}^{(j)} = \mathbf{O}_j[G] - x_{j0}\,\operatorname{grad} G + \mathbf{O}_3[\phi_j] \tag{3.16}$$

and

$$4\pi p^{(j)} = \frac{\partial G}{\partial x_j} + \frac{\partial\phi_j}{\partial z}. \tag{3.17}$$

If we notice that on the plate $z = 0$, $\rho > 1$

$$\mathbf{O}_j[G] = x_j\frac{\partial G}{\partial z}\hat{\mathbf{z}} \quad \text{and} \quad \mathbf{O}_3[\phi] = -\phi\hat{\mathbf{z}} \tag{3.18), (3.19}$$

from their definitions (2.10) and (3.13), then the remaining condition is

$$\phi_j = (x_j - x_{j0})\frac{\partial G}{\partial z} \quad \text{on the plate.} \tag{3.20}$$

Making use of the fact that

$$G - H = \tilde{G} - \tilde{H} = -W^* \tag{3.21}$$

is regular harmonic in the flow field, and $x_j\,\partial\phi/\partial z - z\,\partial\phi/\partial x_j$ is harmonic if $\phi$ is harmonic, $\phi_j$ is easily found to be

$$\phi_j = (x_j - x_{j0})\frac{\partial(G-H)}{\partial z} - z\frac{\partial(G-H)}{\partial x_j}$$

$$= z\frac{\partial W^*}{\partial x_j} - (x_j - x_{j0})\frac{\partial W^*}{\partial z}. \tag{3.22}$$

Unfortunately (3.16) and (3.17) with (3.22) render the velocity ($\rho, z$-component) infinite and the pressure non-integrable at the edge $\xi \to \infty$ (see (3.14)). The singularities on the right-hand-side of (3.16) are found to be (for $j = 1$, 2 and 3):

$$\mathbf{q}'^{(1)} \doteqdot -x_0\mathbf{q}' + \operatorname{Re}\mathbf{q}'^*, \quad \mathbf{q}'^{(2)} \doteqdot \operatorname{Im}\mathbf{q}'^*, \quad \mathbf{q}'^{(3)} \doteqdot -z_0\mathbf{q}', \tag{3.23}$$

where $\doteqdot$ denotes that the terms $O(\mathrm{e}^{-\frac{3}{2}\xi})$ are neglected, and Re and Im denote the real and imaginary parts respectively. Here

$$\left.\begin{aligned} \boldsymbol{q}' &= \mathbf{O}_3\left[\frac{\partial G}{\partial z}\right]+\operatorname{grad} G-\mathbf{O}_3\left[\frac{\partial H}{\partial z}\right] \doteqdot C_G\boldsymbol{q}'_G-C_H\boldsymbol{q}'_H,\\ \boldsymbol{q}'^* &\doteqdot \mathbf{O}_3\left[Z\frac{\partial G}{\partial z}\right]+\operatorname{grad}[ZG]-\mathbf{O}_3\left[Z\frac{\partial H}{\partial z}\right] \doteqdot C_G\boldsymbol{q}'^*_G-C_H\boldsymbol{q}'^*_H,\end{aligned}\right\} \tag{3.24}$$

with

$$C_G = \frac{2}{\pi}M_0\sin\tfrac{1}{2}\eta_0,\quad C_H = \frac{2}{\pi}M_0\cos\tfrac{1}{2}\eta_0, \tag{3.25}$$

$$Z = \mathrm{e}^{\mathrm{i}\theta}, \tag{3.26}$$

$$\begin{aligned} \boldsymbol{q}'_G[\psi] &= \tfrac{1}{2}\mathbf{O}_3[M_c\psi]+\operatorname{grad}\left[\frac{M_s}{M^2}\psi\right],\\ \boldsymbol{q}'_H[\psi] &= \tfrac{1}{2}\mathbf{O}_3[M_s\psi],\\ \boldsymbol{q}'^*_G &= \boldsymbol{q}'_G[\psi Z],\quad \boldsymbol{q}'^*_H = \boldsymbol{q}'_H[\psi Z],\end{aligned} \tag{3.27}$$

and

$$\frac{M_c}{\cos\frac{1}{2}\eta} = \frac{M_s}{\sin\frac{1}{2}\eta} = M(\xi,\eta). \tag{3.28}$$

In these derivations we have made use of (3.14) and the relations

$$\frac{\partial}{\partial z}\left(\frac{M_s}{M^2}\right) = \frac{1}{M}\operatorname{sh}^2\tfrac{1}{2}\xi\cos\tfrac{1}{2}\eta \doteqdot \tfrac{1}{2}M_c \quad\text{and}\quad \frac{\partial}{\partial z}\left(\frac{M_c}{M^2}\right) = \frac{1}{M}\operatorname{ch}^2\tfrac{1}{2}\xi\sin\tfrac{1}{2}\eta \doteqdot \tfrac{1}{2}M_s. \tag{3.29}$$

$\boldsymbol{q}'_G[\psi]$ can be rewritten as

$$\begin{aligned} \boldsymbol{q}'_G[\psi] &\doteqdot \tfrac{1}{3}\mathbf{O}_\rho[M_2\psi]+\tfrac{1}{6}\mathbf{O}_3[M_c\psi]-\tfrac{1}{3}\operatorname{grad}(M_s\psi)\\ &= \tfrac{1}{3}\operatorname{grad}[(\rho-1)M_s\psi]+\tfrac{1}{6}\mathbf{O}_3[M_c\psi]-\tfrac{2}{3}M_s\psi\hat{\boldsymbol{\rho}},\end{aligned} \tag{3.30}$$

where

$$\mathbf{O}_\rho[\Phi] = \rho\operatorname{grad}[\Phi]-\Phi\hat{\boldsymbol{\rho}} \tag{3.31}$$

and we have made use of the relation

$$\begin{aligned} 3\operatorname{grad}\left[\frac{M_s}{M^2}\psi\right] &\doteqdot \mathbf{O}_1[\psi\cos\theta M_s]+\mathbf{O}_2[\psi\sin\theta\, M_s]-\mathbf{O}_3[\psi M_c]-\operatorname{grad}[\psi M_s]\\ &= \mathbf{O}_\rho[\psi M_s]-\mathbf{O}_3[\psi M_c]-\operatorname{grad}[\psi M_s],\end{aligned} \tag{3.32}$$

which can be proved by taking components in cylindrical coordinates and noting (3.29) and the relations

$$\frac{\partial}{\partial\rho}\left(\frac{M_s}{M^2}\right) \doteqdot -\tfrac{1}{2}\rho M_s,\quad \frac{\partial}{\partial\rho}\left(\frac{M_c}{M^2}\right) \doteqdot \tfrac{1}{2}\rho M_c \tag{3.33}$$

as well as

$$\frac{\partial M}{\partial\rho} \doteqdot -\tfrac{1}{2}\rho M^3\cos\eta,\quad \frac{\partial M}{\partial z} \doteqdot -\tfrac{1}{2}zM^3\operatorname{ch}\xi. \tag{3.34}$$

For $\boldsymbol{q}'^*_G$ we have only to replace $\psi$ by $\psi Z$ in the corresponding equations. Our remaining task is to find the Stokes velocities $\boldsymbol{q}$ and $\boldsymbol{q}^*$ vanishing on the plate as analytic continuation of $\boldsymbol{q}'$ and $\boldsymbol{q}'^*$ and subtract them from (3.16).

For this purpose we notice that the harmonic function with $e^{\frac{1}{2}\xi}$ in toroidal coordinates can be expressed as (Bateman 1932)

$$\Phi = M_s\phi \quad \text{or} \quad M_c\phi, \tag{3.35}$$

where

$$\phi = f(\tau Z)+g(\tau \bar{Z}) \tag{3.36}$$

with

$$\tau = \mathrm{th}\,\tfrac{1}{2}\xi, \quad \bar{Z} = \exp(-\mathrm{i}\theta). \tag{3.37}$$

The application to $\boldsymbol{q}'_H$ and $\boldsymbol{q}'^*_H$ is simple. We have only to represent $\psi$ and $\psi Z$ as

$$\psi = \tau_0\tilde{\psi}+1, \quad \psi^* = \psi Z = \tilde{\psi}^*+\tau_0, \tag{3.38), (3.39}$$

where

$$\tilde{\psi} = Zf(Z)+\bar{Z}f(\bar{Z}) \quad \text{and} \quad \tilde{\psi}^* = Zf(Z)+\tau_0^2\bar{Z}f(\bar{Z}) \tag{3.40), (3.41}$$

with

$$f(Z) = \frac{1}{1-\tau_0 Z}, \tag{3.42}$$

Then we have

$$\boldsymbol{q}_H = \tfrac{1}{2}\mathbf{O}_3[M_s\Psi], \quad \boldsymbol{q}^*_H = \tfrac{1}{2}\mathbf{O}_3[M_s\Psi^*], \tag{3.43}$$

where

$$\Psi = \tau_0\tilde{\Psi}+1, \quad \Psi^* = \tilde{\Psi}^*+\tau_0 \tag{3.44}$$

with

$$\tilde{\Psi} = \tau Zf(\tau Z)+\text{c.c.} \tag{3.45}$$

and

$$\tilde{\Psi}^* = \tau Zf(\tau Z)+\tau_0^2\tau\bar{Z}f(\tau\bar{Z}). \tag{3.46}$$

It is easily found that $\boldsymbol{q}_H$ and $\boldsymbol{q}^*_H$ are Stokes velocities vanishing on the wall and yielding the same singularities as $\boldsymbol{q}'_H$ and $\boldsymbol{q}'^*_H$ as $\tau \to 1$, i.e. $\xi \to \infty$.

However, the situations for $\boldsymbol{q}'_G$ and $\boldsymbol{q}'^*_G$ are not simple. If we look for four harmonic functions corresponding to (3.1) and (3.35)–(3.37) in accordance with (3.30), we have for the Stokes velocity

$$\begin{aligned}\boldsymbol{q} &= \mathbf{O}_1[M_s\phi_1]+\mathbf{O}_2[M_s\phi_2]+\mathbf{O}_3[M_c\phi_3]+\operatorname{grad}[M_s\phi_4] \\ &= \mathbf{O}_\rho[M_s\phi_\rho]+2\phi_\theta\hat{\boldsymbol{\theta}}+\mathbf{O}_3[M_c\phi_3]+\operatorname{grad}[M_s\phi_4],\end{aligned} \tag{3.47}$$

with

$$\phi_j = f_j(\tau Z)+g_j(\tau\bar{Z}) \tag{3.48}$$

and

$$\phi_\rho = \cos\theta\,\phi_1+\sin\theta\,\phi_2, \quad \phi_\theta = \sin\theta\,\phi_1-\cos\theta\,\phi_2. \tag{3.49}$$

If we take into account that

$$\frac{\partial M_s}{\partial z} = \pm\tfrac{1}{2}M^3, \quad \rho = \frac{1}{\tau}, \quad M^2 = \mathrm{ch}\,\xi-1 = \frac{2\tau^2}{1-\tau^2} \tag{3.50}$$

on the wall ($\eta = 0, 2\pi$), the condition of vanishing $Q$ on the wall is given by

$$\phi_\rho = \left(\frac{1}{\tau}-\tau\right)\phi_3-\tau\phi_4 \tag{3.51}$$

or

$$f_1 = \left(\frac{1}{\tau Z}-\tau Z\right)f_3-\tau Zf_4, \quad f_2 = \mathrm{i}\left(\frac{1}{\tau Z}+\tau Z\right)f_3+i\tau Zf_4. \tag{3.52}$$

The assumption of $\phi_4 = -\frac{1}{3}\Psi$ and $\phi_3 = \frac{1}{6}\Psi$ with (3.44) in accordance with (3.30) and (3.47) seems to be satisfactory, yielding $\boldsymbol{q}_G[\psi]$ as $\tau \to 1$. Unfortunately, it is singular at $\tau = 0$, i.e. on the $z$-axis, because of the presence of the constant term 1 in (3.44). This difficulty can be easily avoided if we make use of $\tau_0\tilde{\Psi}$ instead of $\Psi$ and complement the axisymmetric part by

$$\boldsymbol{q}_{G0} = \mathbf{O}_3\left[\frac{\partial}{\partial z}\phi_c\right]+\operatorname{grad}\phi_c, \tag{3.53}$$

where

$$\phi_c = \frac{1}{\sqrt{2}}\lambda(1+\zeta\tan^{-1}\zeta) = \frac{M_s}{M^2}+\frac{z}{\sqrt{2}}\tan^{-1}\frac{\sqrt{2}\,M_s}{M^2} \div \frac{M_s}{M^2}, \tag{3.54}$$

corresponding to $\psi = 1$, i.e. the complementary function (multiplied by $2^{-\frac{1}{2}}$) introduced by Hasimoto (1981) to remove the corresponding singularity in the axisymmetric case. Here $\lambda$ and $\zeta$ are ellipsoidal coordinates

$$z = \lambda\zeta, \quad \rho = (1-\lambda^2)^{\frac{1}{2}}(1+\zeta^2)^{\frac{1}{2}} \tag{3.55}$$

related to $\xi$ and $\eta$ by

$$\lambda = \frac{\sqrt{2}\,Ms}{M^2}, \quad \zeta = \frac{\sqrt{2}\,M_c}{M^2}. \tag{3.56}$$

Summarizing, we have

$$\boldsymbol{q}_G = \boldsymbol{q}_{G0}+\tfrac{1}{6}\tau_0\left\{\mathbf{O}_\rho\left[M_s\left(\frac{1}{\tau}+\tau\right)\tilde{\Psi}\right]+\frac{2}{\mathrm{i}}\left(\frac{1}{\tau}-\tau\right)M_s[\tau Zf(\tau Z)-\mathrm{c.c}]\,\hat{\boldsymbol{\theta}}\right.$$
$$\left.+\mathbf{O}_3[M_c\tilde{\Psi}]-2\operatorname{grad}(M_s\tilde{\Psi})\right\} \tag{3.57}$$

and

$$\boldsymbol{q}_G^* = \tau_0\boldsymbol{q}_{GO}+\frac{1}{6}\left\{\mathbf{O}_\rho\left[M_s\left(\frac{1}{\tau}+\tau\right)\tilde{\Psi}^*\right]+\frac{2}{\mathrm{i}}M_s\left(\frac{1}{\tau}-\tau\right)[\tau Zf(\tau Z)-\tau_0^2\tau\bar{Z}f(\tau\bar{Z})]\,\hat{\boldsymbol{\theta}}\right.$$
$$\left.+\mathbf{O}_3[M_c\tilde{\Psi}^*]-2\operatorname{grad}(M_s\tilde{\Psi}^*)\right\}. \tag{3.58}$$

We now have only to add to (3.16) the correction velocities $\boldsymbol{q}^{(j)}$ corresponding to (3.23) and (3.24), using (3.43), (3.57) and (3.58).

Thus the final expression for $\boldsymbol{v}^{(j)}$ satisfying all of the conditions is

$$8\pi\mu\boldsymbol{v}^{(j)} = \mathbf{O}_j[G]-x_{j0}\operatorname{grad}G+\mathbf{O}_3[\phi_j]+\boldsymbol{q}^{(j)}, \tag{3.59}$$

where

$$\boldsymbol{q}^{(1)} = x_0\boldsymbol{q}-\operatorname{Re}\boldsymbol{q}^*, \quad \boldsymbol{q}^{(2)} = -\operatorname{Im}\boldsymbol{q}^*, \quad \boldsymbol{q}^{(3)} = z_0\boldsymbol{q}, \tag{3.60}$$

with

$$\boldsymbol{q} = C_G\boldsymbol{q}_G-C_H\boldsymbol{q}_H, \quad \boldsymbol{q}^* = C_G\boldsymbol{q}_G^*-C_H\boldsymbol{q}_H^*. \tag{3.61}$$

By use of (3.1) and (3.2), the vorticities $\boldsymbol{\omega}^{(j)}$ and the pressure corresponding to (3.61) are given by

$$4\pi\mu\boldsymbol{\omega}^{(j)} = \hat{\boldsymbol{x}}_j\times\operatorname{grad}G+\hat{\boldsymbol{x}}_3\times\operatorname{grad}\phi_j+\boldsymbol{\nu}^{(j)} \tag{3.62}$$

and

$$4\pi p^{(j)} = \frac{\partial}{\partial x_j}G+\frac{\partial}{\partial x_3}\phi_j+\pi^{(j)}, \tag{3.63}$$

where

$$\left.\begin{aligned} \boldsymbol{\nu}^{(1)} &= x_0\boldsymbol{\nu}-\mathrm{Re}\,\boldsymbol{\nu}^*, \quad \pi^{(1)} = x_0\pi-\mathrm{Re}\,\pi^*,\\ \boldsymbol{\nu}^{(2)} &= -\mathrm{Im}\,\boldsymbol{\nu}^*, \quad \pi^{(2)} = -\mathrm{Im}\,\pi^*,\\ \boldsymbol{\nu}^{(3)} &= z_0\boldsymbol{\nu}, \quad \pi^{(3)} = z_0\pi, \end{aligned}\right\} \tag{3.64}$$

with

$$\left.\begin{aligned} \boldsymbol{\nu} &= C_G\boldsymbol{\nu}_G-C_H\boldsymbol{\nu}_H, \quad \pi = C_G\pi_G-C_H\pi_H,\\ \boldsymbol{\nu}^* &= C_G\boldsymbol{\nu}_G^*-C_H\boldsymbol{\nu}_H^*, \quad \pi^* = C_G\pi_G^*-C_H\pi_H^*. \end{aligned}\right\} \tag{3.65}$$

where

$$\left.\begin{aligned} \boldsymbol{\nu}_G &= \hat{\boldsymbol{x}}_3\times\mathrm{grad}\frac{\partial}{\partial z}\phi_c+\tfrac{1}{6}\tau_0\left[\hat{\boldsymbol{\rho}}\times\mathrm{grad}\left[M_s\left(\frac{1}{\tau}+\tau\right)\tilde{\Psi}\right]\right.\\ &\quad\left.+\frac{\hat{\boldsymbol{\theta}}}{\rho}\times\mathrm{grad}\left[\mathrm{i}\rho M_s\left(\frac{1}{\tau}-\tau\right)[\tau Zf(\tau Z)-\mathrm{c.c.}]\right]+\hat{\boldsymbol{x}}_3\times\mathrm{grad}\,[M_c\tilde{\Psi}]\right],\\ \boldsymbol{\nu}_G^* &= \tau_0\hat{\boldsymbol{x}}_3\times\mathrm{grad}\frac{\partial}{\partial z}\phi_c+\frac{1}{6}\left[\hat{\boldsymbol{\rho}}\times\mathrm{grad}\left[M_s\left(\frac{1}{\tau}+\tau\right)\tilde{\Psi}^*\right]\right.\\ &\quad\left.+\frac{\hat{\boldsymbol{\theta}}}{\rho}\times\mathrm{grad}\left[\mathrm{i}\rho M_s\left(\frac{1}{\tau}-\tau\right)[\tau Zf(\tau Z)-\tau_0^2\tau\bar{Z}f(t\bar{Z})]\right]+\hat{\boldsymbol{x}}_3\times\mathrm{grad}\,[M_c\tilde{\Psi}^*]\right],\\ \pi_G &= \frac{\partial^2}{\partial z^2}\phi_c+\frac{\tau_0}{6}\left[\left(\frac{\partial}{\partial\rho}+\frac{1}{\rho}\right)\left[M_s\left(\frac{1}{\tau}+\tau\right)\tilde{\Psi}\right]+\frac{1}{\rho}\frac{\partial}{\partial\theta}\left[\mathrm{i}M_s\left(\frac{1}{\tau}-\tau\right)[\tau Zf(\tau Z)-\mathrm{c.c.}]\right]\right.\\ &\quad\left.+\frac{\partial}{\partial z}[M_c\tilde{\Psi}]\right],\\ \pi_G^* &= \tau_0\frac{\partial^2}{\partial z^2}\phi_c+\frac{1}{6}\left[\left(\frac{\partial}{\partial\rho}+\frac{1}{\rho}\right)\left[M_s\left(\frac{1}{\tau}+\tau\right)\tilde{\Psi}^*\right]\right.\\ &\quad\left.+\frac{1}{\rho}\frac{\partial}{\partial\theta}\left[\mathrm{i}M_s\left(\frac{1}{\tau}-\tau\right)\left[\tau Zf(\tau Z)-\tau_0^2\tau\bar{Z}f(\tau\bar{Z})\right]\right]+\frac{\partial}{\partial z}[M_c\tilde{\Psi}^*]\right]. \end{aligned}\right\} \tag{3.66}$$

In these expressions

$$\tilde{\Psi} = \frac{\tau_0 z}{1-\tau_0\tau z}+\mathrm{c.c.} = \frac{\tau}{H}(2\cos\theta-\tau_0\tau) \tag{3.67}$$

and

$$\begin{aligned} \tilde{\Psi}^* &= \frac{\tau z}{1-\tau_0\tau z}+\frac{\tau_0^2\tau\bar{z}}{1-\tau_0\tau\bar{z}} \\ &= \frac{\tau}{H}[2(1+\tau_0^2)\cos\theta-\tau_0(1+\tau_0^2)+2\mathrm{i}(1-\tau_0^2)\sin\theta], \end{aligned} \tag{3.68}$$

with

$$H = 1-2\tau_0\tau\cos\theta+\tau_0^2\tau^2, \tag{3.69}$$

where we have made use of (3.40)–(3.42).

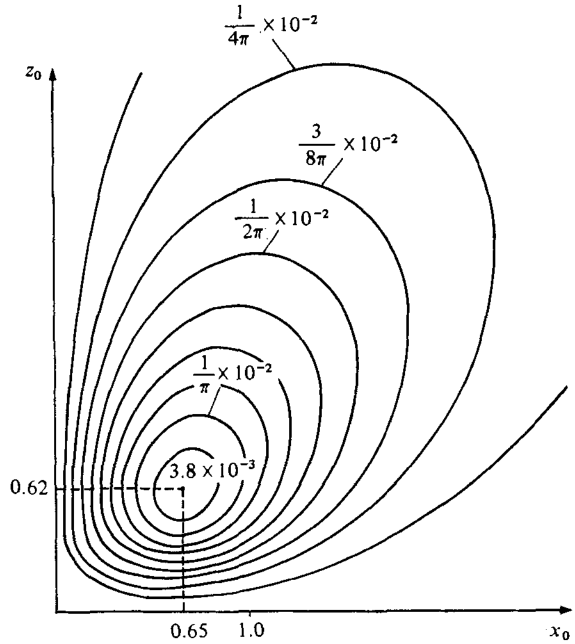


FIGURE 2. Volume flux induced by the radial translation of the sphere; as contours in the $(x_0, z_0)$-plane.

## 4. Translation of a small sphere

### 4.1. *Volume flux through the hole*

When a small sphere of radius $a$ translates with the velocity $\boldsymbol{U} = \Sigma_{j=1}^{3} U^{(j)}\hat{\boldsymbol{x}}_j$, a net volume flux $Q$ through the hole is induced. To the lowest order of $a$ we have

$$Q = -D_0 \boldsymbol{Q}^{\mathrm{t}} \cdot \boldsymbol{U}, \tag{4.1}$$

where

$$D_0 = 6\pi\mu a, \tag{4.2}$$

$$\boldsymbol{Q}^{\mathrm{t}} = (Q^{(1)}, Q^{(2)}, Q^{(3)}), \tag{4.3}$$

$$Q^{(j)} = \int_0^{2\pi}\int_0^1 v_3^{(j)}(\rho,\theta,0)\,\rho\,\mathrm{d}\rho\,\mathrm{d}\theta. \tag{4.4}$$

Equation (4.4) integrates to zero for $j = 2$, because of symmetry. The contours in the $(x_0, z_0)$-plane of $Q^{(1)}$ and $Q^{(3)}$ are shown in figures 2 and 3 respectively.

$Q^{(1)}$ takes the maximum value $Q_{\mathrm{M}}^{(1)} = 3.8\times 10^{-3}$ at $P_{\mathrm{M}}^{(1)}$ (0.65, 0.62), vanishing on both axes and at infinity.

$Q^{(3)}$ takes the maximum value $Q_{\mathrm{M}}^{(3)} = 1.6\times 10^{-1}$ at the origin. It decreases slowly in the $z_0$ direction and rapidly in the $x_0$ direction.

Note that there is at any position in the $(x_0, z_0)$-plane one direction along which the sphere translates giving no volume flux; e.g. $-2.8°$ to the $x_0$ axis at $P_{\mathrm{M}}^{(1)}$ (0.65, 0.62).

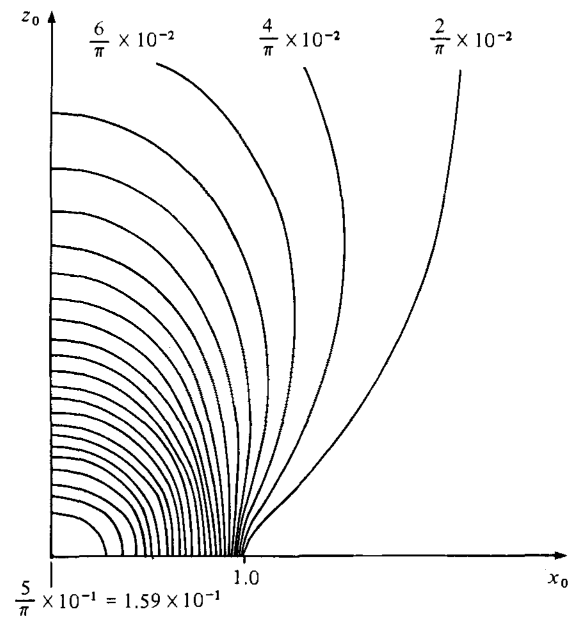


FIGURE 3. Volume flux induced by the axial translation of the sphere; as contours in the $(x_0, z_0)$-plane.

## 4.2. *Drag, sideforce and torque*

We can evaluate the force $\boldsymbol{F}^{(j)}$ and torque $\boldsymbol{T}^{(j)}$ acting on the sphere translating parallel to each axis with the velocity $U^{(j)}\hat{\boldsymbol{x}}_j$ to the first order in the wall effect, by means of the generalized Faxen law (see e.g. Happel & Brenner 1965):

$$\boldsymbol{F}^{(j)} = -D_0 U^{(j)}\hat{\boldsymbol{x}}_j + D_0 \left\langle \boldsymbol{v}^{(j)} - \frac{\boldsymbol{q}_{\mathrm{S}}^{(j)}}{8\pi\mu} \right\rangle_0, \tag{4.5}$$

$$\boldsymbol{T}^{(j)} = -\tfrac{2}{3}a^2 D_0 \left\langle \boldsymbol{\omega}^{(j)} - \frac{\boldsymbol{\omega}_{\mathrm{S}}^{(j)}}{8\pi\mu} \right\rangle_0, \tag{4.6}$$

where

$$\boldsymbol{w}_{\mathrm{S}}^{(j)} = \operatorname{curl} \boldsymbol{q}_{\mathrm{S}}^{(j)} = 2\hat{\boldsymbol{x}}_j \times \operatorname{grad}(1/R) \tag{4.7}$$

and $\langle \quad \rangle_0$ implies the induced field evaluated at the centre of the sphere $x = x_0$ with the subtraction of the fields $\boldsymbol{q}_{\mathrm{S}}^{(j)}$ and $\boldsymbol{\omega}_{\mathrm{S}}^{(j)}$ of the Stokeslet.

Evaluating the value at the position $x_0$, we have

$$\boldsymbol{F} = -6\pi\mu a[\boldsymbol{I} + a\boldsymbol{K} + O(a^2)]\cdot \boldsymbol{U}$$

and

$$\boldsymbol{T} = -8\pi\mu a^2[a^2\boldsymbol{C} + O(a^4)]\cdot \boldsymbol{U},$$

where $\boldsymbol{I}$ is the unit tensor and

$$\boldsymbol{K} = \begin{pmatrix} f_{xx} & 0 & f_{xz} \\ 0 & f_{yy} & 0 \\ f_{zx} & 0 & f_{zz} \end{pmatrix}, \quad \boldsymbol{C} = \begin{pmatrix} 0 & t_{xy} & 0 \\ t_{yx} & 0 & t_{yz} \\ 0 & t_{zy} & 0 \end{pmatrix}, \tag{4.8}$$

with

$$\left.\begin{aligned}
f_{xx} &= \frac{1}{16\pi}\left[M^2\left(9\frac{\pi-\eta}{\sin\eta}+6-6\cos\eta+8\cos^2\eta+\cos^3\eta\right)\right.\\
&\quad +2(1-\cos\eta)(3+\cos\eta-5\cos^2\eta-\cos^3\eta)\\
&\quad \left.-\frac{1+\cos\eta}{M^2}\sin^2\eta\left(\frac{4}{\operatorname{ch}\xi+1}-2-\cos\eta+\cos^2\eta\right)\right]\\
f_{zx} &= f_{xz} = \frac{\operatorname{sh}\xi\sin\eta}{16\pi M^2}(1-\cos\eta)\left[\frac{4(1+\cos\eta)}{\operatorname{ch}\xi+1}-\operatorname{ch}\xi\cos\eta-9\operatorname{ch}\xi+8\cos\eta-2\right]\\
f_{zz} &= \frac{1}{16\pi}\left[M^2\left(\frac{18(\pi-\eta)}{\sin\eta}+6\right)-12(1-\operatorname{ch}\xi\cos\eta)\right.\\
&\quad \left.+\frac{\sin^2\eta}{M^2}(\operatorname{ch}^2\xi\cos\eta+8M^2\operatorname{ch}\xi+2\operatorname{ch}\xi-5\cos\eta+2)\right],\\
f_{yy} &= \frac{M^2}{16\pi}\left[\frac{8(1-\cos\eta)}{\operatorname{ch}\xi+1}+\frac{9(\pi-\eta)}{\sin\eta}+8+\cos\eta\right]
\end{aligned}\right\} \tag{4.9}$$

and

$$\left.\begin{aligned}
t_{yx} &= -\frac{1}{16\pi}(\operatorname{ch}\xi-1)\sin\eta\left[\operatorname{ch}\xi\cos\eta+3\operatorname{ch}\xi-2\cos\eta+2-\frac{4(1+\cos\eta)}{\operatorname{ch}\xi+1}\right],\\
t_{xy} &= \frac{1}{16\pi}M^2\tau^2\sin\eta\,(\operatorname{ch}\xi-1) = \frac{1}{16\pi}M^4\tau^2 z\,(\operatorname{ch}\xi-1),\\
t_{zy} &= \frac{1}{16\pi}M^2\tau^2\operatorname{sh}\xi(1-\cos\eta) = \frac{1}{16\pi}M^4\tau^2\rho(1-\cos\eta),\\
t_{yz} &= -\frac{1}{16\pi}\operatorname{sh}\xi\,(1-\cos\eta)\,[3M^2+\tau^2(\operatorname{ch}\xi+2)(1+\cos\eta)].
\end{aligned}\right\} \tag{4.10}$$

Here we have omitted the suffixes 0 from $\xi_0$, $\eta_0$ and $M_0$ for the sake of brevity.

The tensor $\boldsymbol{C}$ is useful in predicting the angular velocity $\boldsymbol{\Omega}$ of the sphere when it is allowed to rotate (Sano & Hasimoto 1978):

$$\boldsymbol{\Omega} = -\boldsymbol{C}\cdot Ia+O(a^4), \tag{4.11}$$

the effect of rotation on the force being of higher order.

Let us begin with two special positions of the sphere (i) on the $z$-axis; and (ii) on the aperture. When the sphere is on the $z$-axis, i.e. $\xi_0 = 0$, we have

$$\left.\begin{aligned}
f_{xx} = f_{yy} &= \frac{3}{16\pi}(1-\cos\eta_0)\left(4-\cos\eta_0+\frac{3(\pi-\eta_0)}{\sin\eta_0}\right)\\
&= \frac{9}{8\pi}\frac{\tan^{-1}z_0}{z_0}+\frac{3}{8\pi}\left(\frac{3}{1+z_0^2}+\frac{2}{(1+z_0^2)^2}\right),\\
f_{zz} &= \frac{3}{8\pi}(1-\cos\eta_0)\left(1+2\cos\eta_0+\frac{3(\pi-\eta_0)}{\sin\eta_0}\right)\\
&= \frac{9}{4\pi}\frac{\tan^{-1}z_0}{z_0}+\frac{3}{4\pi}\left(\frac{3}{1+z_0^2}-\frac{4}{(1+z_0^2)^2}\right),\\
f_{xz} &= f_{zx} = 0, \quad \boldsymbol{C} = 0.
\end{aligned}\right\} \tag{4.12}$$

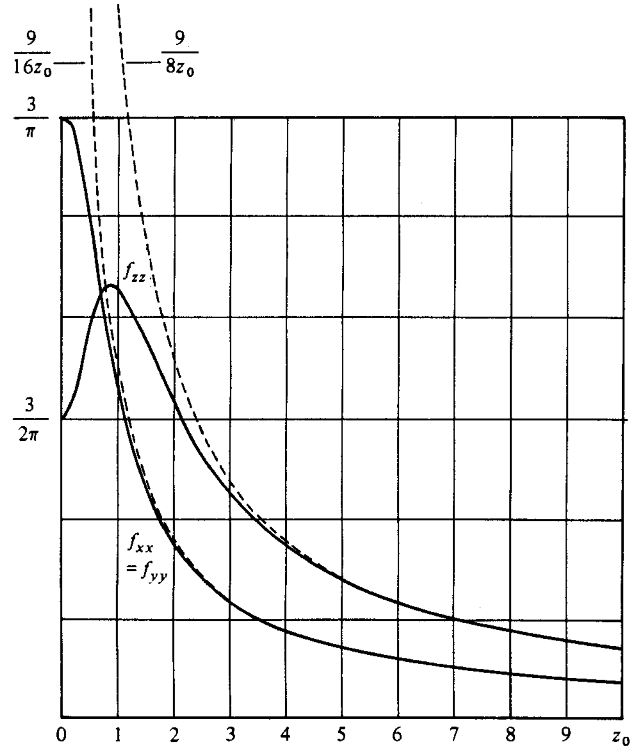


FIGURE 4. Variation of $f_{xx} = f_{yy}$ and $f_{zz}$ when the sphere is on the $z$-axis.

The formula for $f_{zz}$ in (4.12) has already been given by Hasimoto (1979, 1981) and Davis *et al.* (1981). Figure 4 shows the variation of $f_{xx} = f_{yy}$ with respect to $z_0$. Note that $f_{zz}$ has an extremum 0.69 at $z_0 = 0.8702$, in contrast with $f_{xx} = f_{yy}$, which decreases monotonically as $z_0$ increases. If we consider the symmetry, we are sure that $f_{xz} = f_{zx}$, $t_{zy}$, $t_{yz}$ and $t_{xy} + t_{yx}$ must vanish on the axis. However, the vanishing of $t_{xy}$ to the lowest order of approximation is a little surprising.

When the sphere is on the aperture, i.e. $\eta_0 = \pi$, we have

$$\left.\begin{aligned} f_{xx} &= \frac{1}{4\pi}(7\operatorname{ch}\xi_0 + 5) = \frac{1}{2\pi}\frac{6+x_0^2}{1-x_0^2}, \\ f_{yy} &= \frac{1}{\pi}(\operatorname{ch}\xi_0 + 2) = \frac{1}{\pi}\frac{3-x_0^2}{1-x_0^2}, \\ f_{zz} &= \frac{3}{4\pi}(\operatorname{ch}\xi_0 + 1) = \frac{3}{2\pi}\frac{1}{1-x_0^2}, \\ t_{zy} &= \frac{1}{8\pi}\operatorname{sh}\xi_0(\operatorname{ch}\xi_0 - 1) = \frac{1}{2\pi}\frac{x_0^3}{(1-x_0^2)^2}, \\ t_{yz} &= -\frac{3}{8\pi}\operatorname{sh}\xi_0(\operatorname{ch}\xi_0 + 1) = -\frac{3}{2\pi}\frac{x_0}{(1-x_0^2)^2}. \end{aligned}\right\} \qquad (4.13)$$

The variations of $f_{xx}$, $f_{yy}$ and $f_{zz}$ with respect to $x_0$ are shown in figure 5, and those

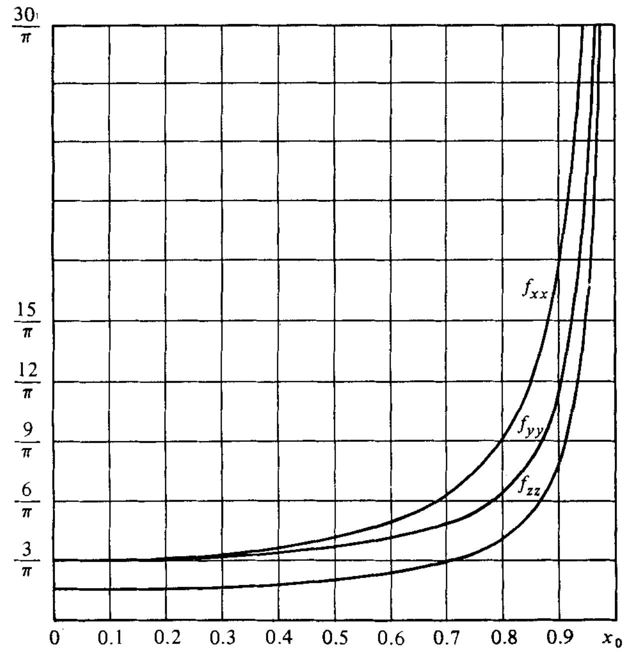


FIGURE 5. Variation of $f_{xx}$, $f_{yy}$ and $f_{zz}$ when the sphere is in the aperture.

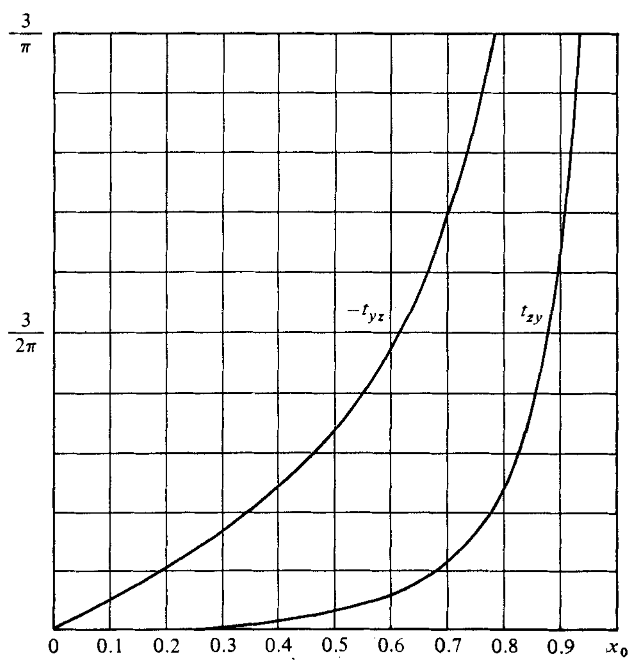


FIGURE 6. Variation of $t_{yz}$ and $t_{zy}$ when the sphere is in the aperture.

of $t_{zy}$ and $t_{yz}$ in figure 6. As the edge is approached, they increase monotonically to the limits satisfying the relation

$$f_{xx}:f_{yy}:f_{zz} = 7:4:3, \qquad t_{zy}:t_{yz} = 1:-3. \tag{4.14}$$

The same relation is found in the case of a semi-infinite plane (Hasimoto *et al.* 1983).

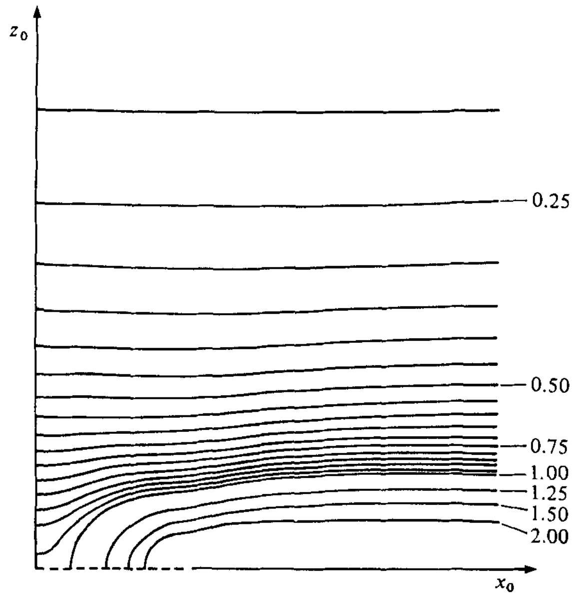


FIGURE 7. Contours of $f_{xx}$ in the $(x_0, z_0)$-plane.

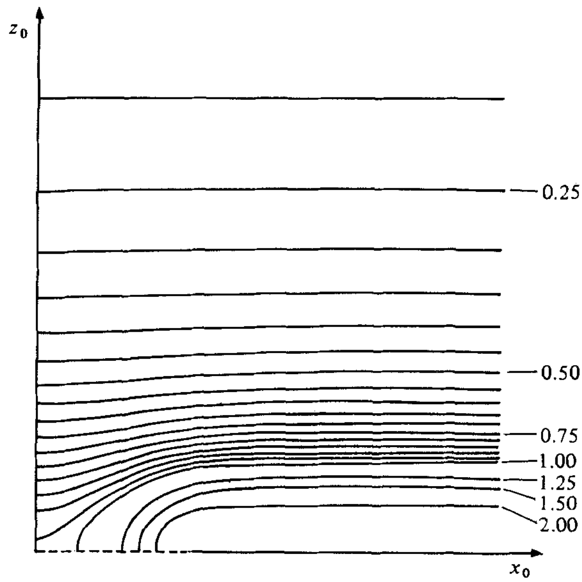


FIGURE 8. Contours of $f_{yy}$ in the $(x_0, z_0)$-plane.

In fact, taking the limit $\xi_0 \to \infty$ in (4.9) and (4.10), we have the same expressions as in the case of a semi-infinite plane. On the other hand, at the centre $\rho_0 = 0$, we have

$$f_{xx} : f_{yy} : f_{zz} = 2:2:1, \quad t_{zy} = t_{yz} = 0. \tag{4.15}$$

When the sphere is at any position in the $(x_0, z_0)$-plane the diagonal elements of $\boldsymbol{K}$ represent the drag correction, which is always positive. Contours of $f_{xx}$, $f_{yy}$ and $f_{zz}$ are given in figure 7, 8 and 9 respectively. The anisotropy of $\boldsymbol{K}$ causes a sideforce when the sphere translates along a line that is skewed with respect to the coordinate axes. It is interesting to note that the extremum value of $f_{xx}$ at $x_0 = 0$ for fixed $z_0$

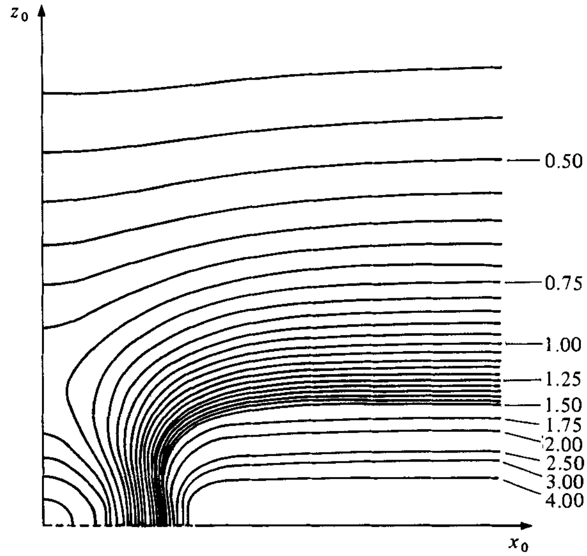


FIGURE 9. Contours of $f_{zz}$ in the $(x_0, z_0)$-plane.

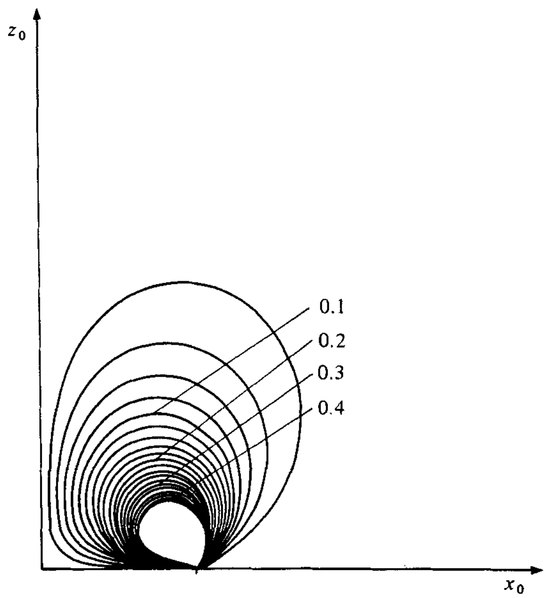


FIGURE 10. Contours of $f_{xz} = f_{zx}$ in the $(x_0, z_0)$-plane.

is not always a local minimum; i.e. maximum for $z_0 > 1.08$. This effect will be investigated in detail when the sphere moves on the plane of fixed height $z_0$.

The off-diagonal parts also imply the presence of sideforce even in translation parallel to the $z$ or radial axis. Contours of $f_{xz} = f_{zx}$ are shown in figure 10. When the sphere approaches the plane in a direction parallel to the $z$-axis, there is an inward sideforce. When the sphere moves in the radial direction outward, there is an upward sideforce. No sideforce appears when the sphere translates in the azimuthal direction, as is clear from symmetry considerations.

As an example of the translation of the sphere experiencing composite forces, we

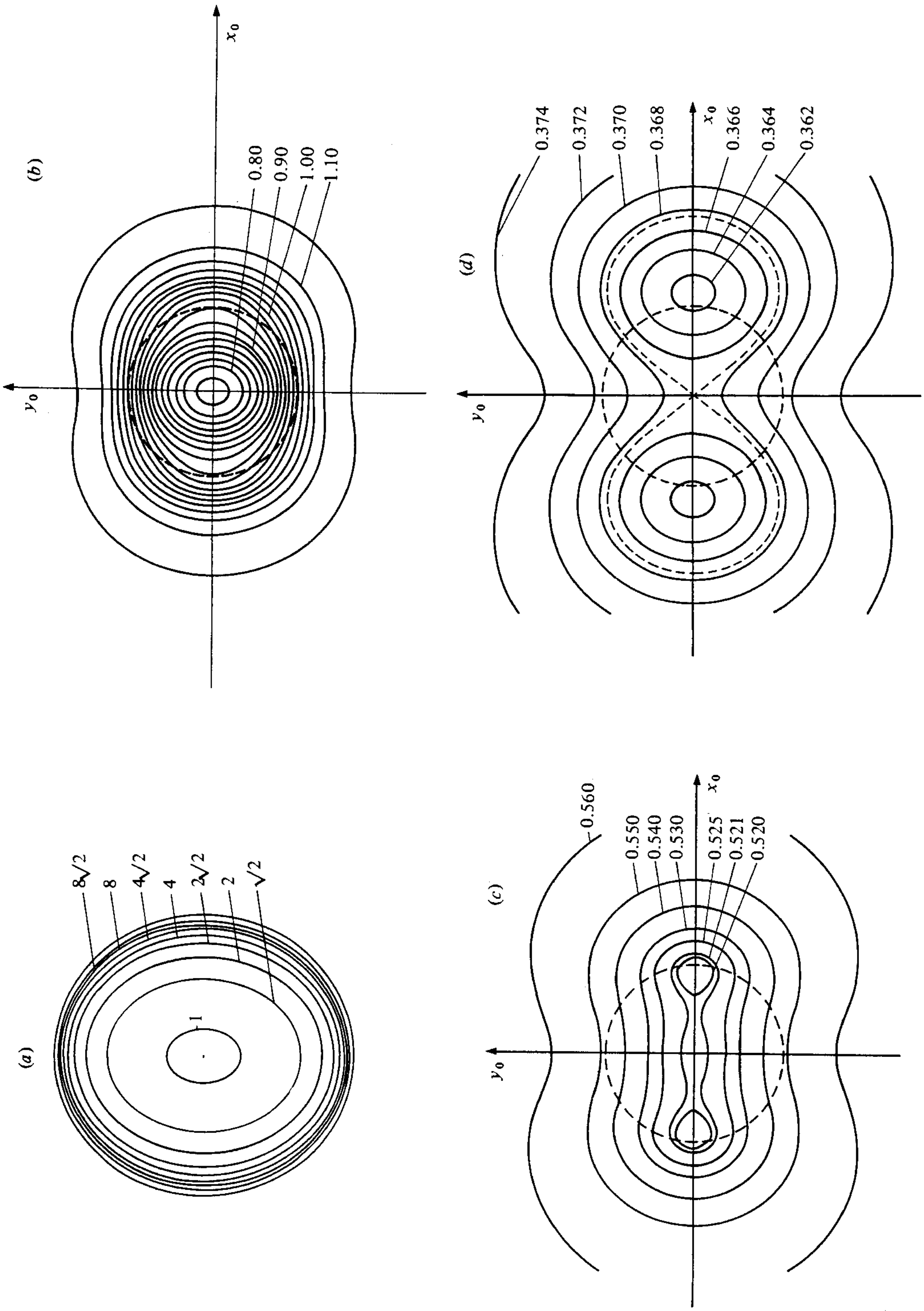


FIGURE 11. Contours of the drag correction in the $(x_0, y_0)$-plane when the sphere translates parallel to the $x$-axis for fixed $z_0$; (*a*) $z_0 = 0$; (*b*) 0.5; (*c*) 1.0; (*d*) = 1.5.

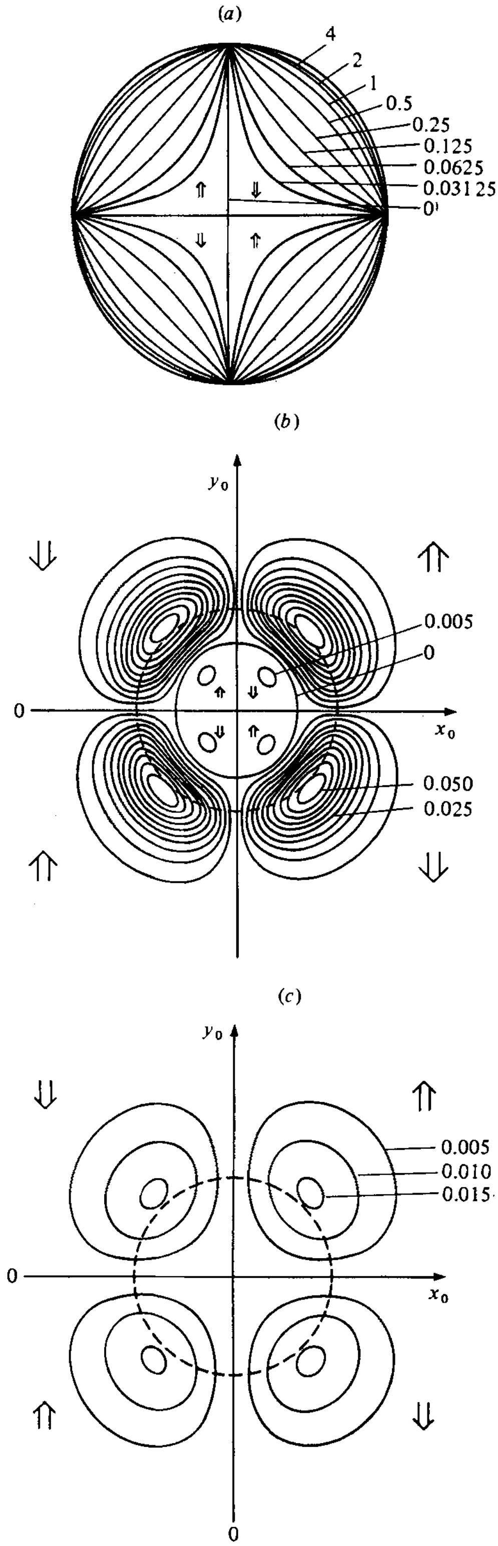


FIGURE 12. Contours of the sideforce ($y$-component) in the $(x_0, y_0)$-plane when the sphere translates parallel to the $x$-axis for fixed $z_0$: ($a$) $z_0 = 0$; ($b$) 0.5; ($c$) 1.0.

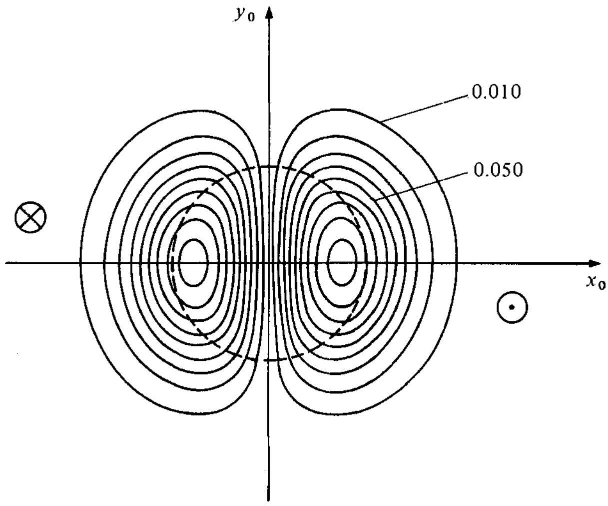


FIGURE 13. Contours of the sideforce ($z$-component) in the $(x_0, y_0)$-plane when the sphere translates parallel to the $x$-axis for fixed $z_0$ $(= 1.0)$.

consider motion parallel to the $x$-axis for fixed $z_0$ and $y_0$. Figure 11 shows the contour of drag correction $(-F_x/D_0 - 1)/a$ for $z_0 = 0$, 0.5, 10 and 1.5 (figures 11 *a, b, c, d*).

Note the topological differences between figures 11 (*c*) and (*d*). In figure 11 (*c*) the minimum value is attained at the origin $(x_0 = y_0 = 0)$, but in figure 11 (*d*) the origin becomes the local saddle point, which has already been expected from examination of figure 7. This result seems to be related to the fact that the maximum induced volume flux is attained at $(0.65, 0.62)$ in the $(x_0, z_0)$-plane; the reduction of drag correction by the induced flow being rather larger off-axis and off-plane. We note that these topological changes take place at $z_0 = 0.88$ and 1.08. The influence of the hole vanishes rapidly as $y_0$ is increased.

Figures 12 and 13 show the contours of sideforce $F_y/D_0 a$ and $F_z/D_0 a$ respectively. The sideforce $F_y/D_0 a$ is due to the anisotropy of the tensor $\boldsymbol{K}$. It shows a very interesting variation when the sphere moves along the line $y_0 =$ const. In figure 12 (*b*) $F_y/D_0 a$ changes its sign three times if $|y_0| < 0.64$, first (inward $\rightarrow$ outward) when the sphere enters the semicircle of radius 0.64 from negative $x_0$, secondly (outward $\rightarrow$ inward) at $x_0 = 0$, and finally (inward $\rightarrow$ outward) at the opposite semicircle. Whereas for $|y_0| \geqslant 0.64$ the change occurs only at $x_0 = 0$, similarly to the case of greater height $|z_0| \geqslant 0.74$, where the change occurs only once for any value of $y_0$ (figure 12 *c*).

The sideforce $F_z/D_0 a$ is due to the off-diagonal components of $\boldsymbol{K}$. Its sign change takes place at $x_0 = 0$ (downward $\rightarrow$ upward). The influence of the hole is small, except for a small region near the hole. In particular $F_z/D_0 a$ decreases very rapidly, and the force correction to the sphere is nearly parallel to the plane when it moves far off-axis.

Contours of the torque $t_{xy}$, $t_{yx}$, $t_{yz}$ and $t_{zy}$ in the $(x_0, z_0)$ $(z_0 > 0)$ plane are given in figures 14, 15, 16 and 17 respectively.

The values of $t_{xy}$ and $t_{yx}$ vanish on both axes to our order of approximation, as in the case of a rigid wall, where they are $O(a^4)$. When the sphere moves in the radial off-axis direction, a positive azimuthal component of torque appears. When the sphere moves in the positive azimuthal direction, a negative radial component of torque occurs. These torques increase to infinity as the edge is approached. The values of $t_{yz}$ and $t_{zy}$ vanish on the $z_0$ axis and on the rigid wall, as is to be expected from the symmetry of the problem. The torque of the positive azimuthal component

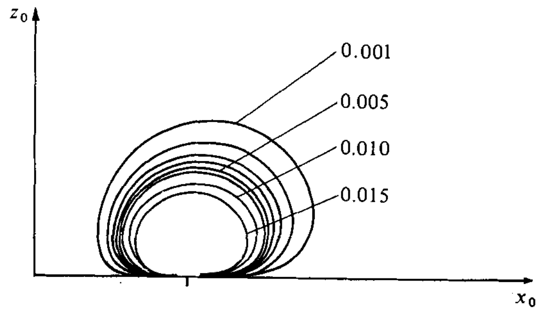


FIGURE 14. Contours of $t_{xy}$ in the $(x_0, z_0)$-plane.

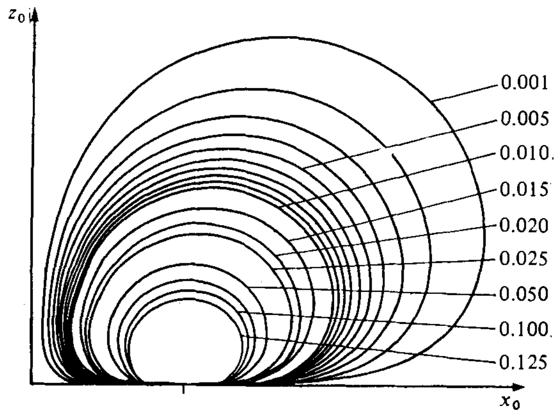


FIGURE 15. Contours of $-t_{yx}$ in the $(x_0, z_0)$-plane.

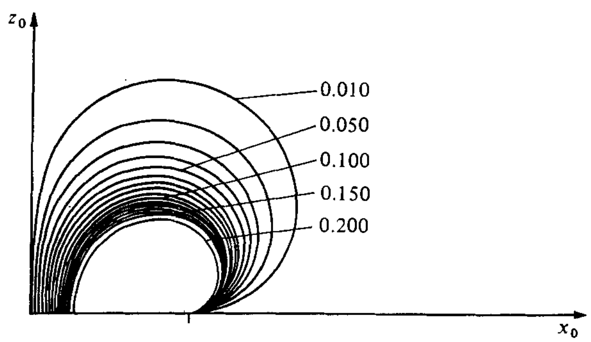


FIGURE 16. Contours of $-t_{yz}$ in the $(x_0, z_0)$-plane.

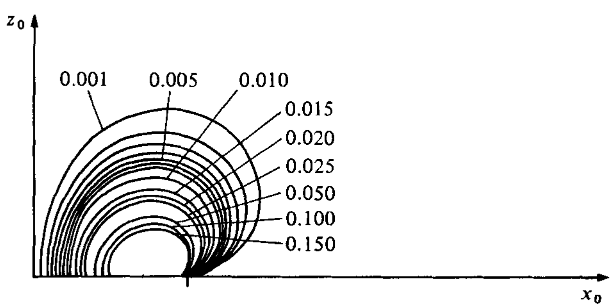


FIGURE 17. Contours of $t_{zy}$ in the $(x_0, z_0)$-plane.

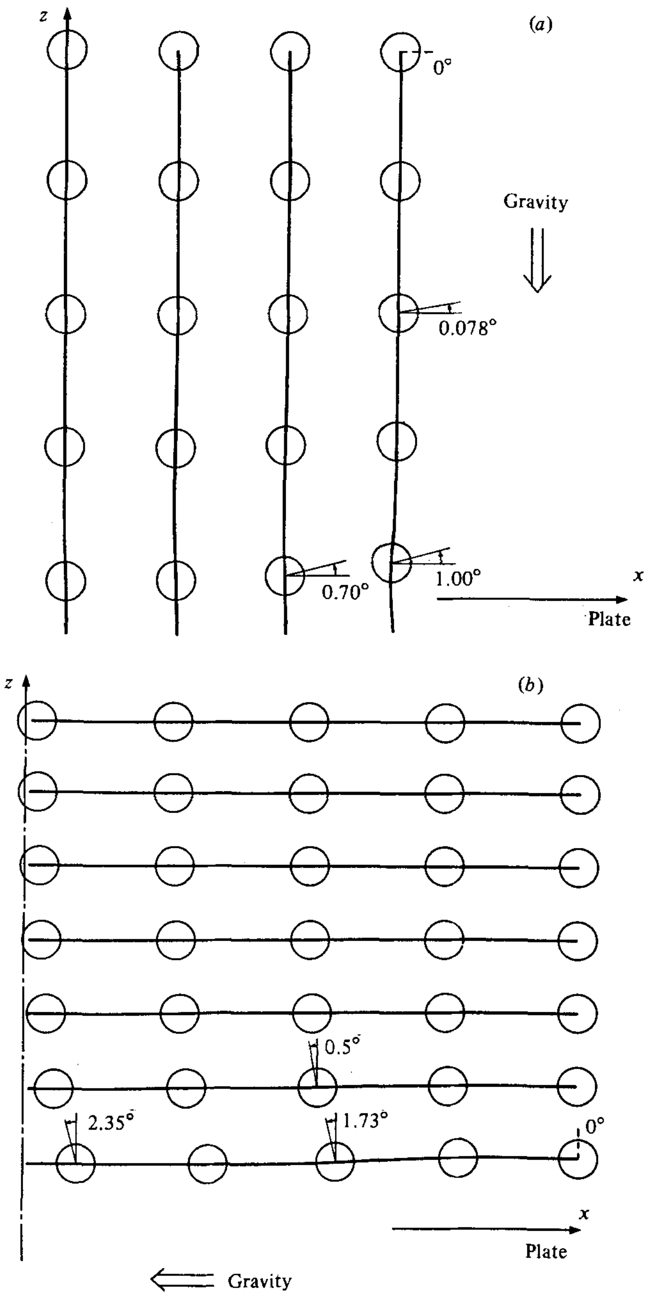


FIGURE 18. Trajectories of a small sphere: (a) through a hole in a horizontal wall; (b) beside a vertical wall with a hole.

appears when the sphere moves in the positive $z$-direction. Torque around the negative $z$-axis occurs when the sphere moves in the positive azimuthal direction. They increase infinitely as we approach the edge of the hole, where the asymptotic form given in the case of the semi-infinite plane is attained. For $z_0 < 0$ we have only to notice that $t_{xy}$ and $t_{yx}$ are odd functions of $z_0$ and that $t_{yz}$ and $t_{zy}$ are even.

As an application of our results, the trajectories of a small sphere (diameter 0.1) under the effect of constant gravity are calculated for two cases:

($a$) when the sphere is dropped through a hole in a horizontal wall;
($b$) when the sphere is dropped besides a vertical wall with a hole.

Figure 18($a$) shows the trajectories for case ($a$), where a gravitational force with negative $z$-component acts on the sphere. The initial positions of the sphere are $(x, y, z) = (0,\ 0,\ 1.5)$, $(0.3, 0, 1.5)$, $(0.6, 0, 1.5)$ and $(0.9, 0, 1.5)$. The trajectories for case ($b$) are given in figure 18($b$), where gravity, parallel to the negative $x$-axis, is exerted on the sphere. The initial positions are $(1.5, 0, 0.2)$, $(1.5, 0, 0.4)$ and $(1.5, 0, 1.4)$. All trajectories remain in the $(x, z)$-plane, and the subsequent positions of the sphere are shown in the figures. When the sphere moves near the plane wall, its translational velocity decreases, because it suffers larger drag. The effect of the sideforce is remarkable in the vicinity of the edge. The arrow signs in the figures represent the rotation of the sphere. Note that the rotational velocity is so small that the effect on the force is negligible in our approximation.

The authors would like to express their thanks to Dr A. M. J. Davis for making them aware of his study on the same subject (Davis 1983). In his paper, the mixed boundary-value problem is reduced to a dual integral equation and the solution is given in the form of infinite series of integrals.

This work is partially supported by a Grant-in-Aid for Scientific Research from the Ministry of Education.

## REFERENCES

BATEMAN, H. 1932 *Partial Differential Equations*, p. 461. Cambridge University Press.

BRENNER, H. 1964 *J. Fluid Mech.* **18**, 144.

DAGAN, Z., WEINBAUM, S. & PFEFFER, R. 1982 *J. Fluid Mech.* **117**, 143.

DAVIS, A. M. J. 1983 *Intl J. Multiphase Flow* **9**, 575.

DAVIS, A. M. J., O'NEILL, M. E. & BRENNER, H. 1981 *J. Fluid Mech.* **103**, 183 (and Corrigendum **111**, 1981, 499).

HAPPELL, J. & BRENNER, H. 1965 *Low Reynolds Number Hydrodynamics*, chaps 5 and 7. Prentice-Hall.

HASIMOTO, H. 1978 Mixed boundary value problem in fluid mechanics. *Inst. Math. Sci. Kyoto Univ. Lecture Note* 335, *p*. 1. (In Japanese)

HASIMOTO, H. 1979 Mixed boundary value problem in fluid mechanics. *Inst. Math. Sci. Kyoto Univ. Lecture Note* 360, p. 1. (In Japanese)

HASIMOTO, H. 1981 *J. Phys. Soc. Japan* **50**, 4068.

HASIMOTO, H., KIM, M. & MIYAZAKI, T. 1983 *J. Phys. Soc. Japan* **52**, 1996.

HASIMOTO, H. & SANO, O. 1980 *Ann. Rev. Fluid Mech.* **12**, 335.

IMAI, I. 1973 *Ryutai Rikigaku* (*Fluid Mechanics*), Tokyo p. 428 Syokabo. (In Japanese)

KIM, M. 1979 *J. Phys. Soc. Japan* **47**, 1670.

MIYAZAKI, T. & HASIMOTO, H. 1982 *J. Phys. Soc. Japan* **51**, 2343.

SANO, O. & HASIMOTO, H. 1976 *J. Phys. Soc. Japan* **40**, 884.

SANO, O. & HASIMOTO, H. 1977 *J. Phys. Soc. Japan* **42**, 306.

SANO, O. & HASIMOTO, H. 1978 *J. Fluid Mech.* **87**, 673.

WENDT, G. 1958 In *Handbuch der Physik* (ed. S. Flugge), vol. 16, p. 144. Springer.